# EPMA and TEM investigations on the interdiffusion layer of the PNN/PZT functionally gradient piezoelectric ceramics

XINHUA ZHU*, JIANMIN ZHU, SHUNHUA ZHOU, QI LI,
ZHIGUO LIU, NAIBEN MING
*National Laboratory of Solid State of Microstructures, Department of Physics,
Nanjing University, Nanjing 210093, People's Republic of China*

ZHONGYAN MENG
*School of Materials Science and Engineering, Shanghai University (Jiading Campus),
Shanghai 201800, People's Republic of China*
E-mail: liqi@netra.nju.edu.cu

The compositional profile, distribution of the phases and the ordering behavior in the interdiffusion layer of the PNN/PZT functionally gradient piezoelectric ceramics have been investigated by electron probe microbeam analyses (EPMA) and transmission electron microscopy (TEM) respectively. The results show that the thickness of the interdiffusion layers ($d$) for $Ni^{2+}$, $Nb^{5+}$, $Ti^{4+}$ and $Zr^{4+}$ ions are ordered as $d_{Ni}^{2+} > d_{Nb}^{5+} > d_{Ti}^{4+} > d_{Zr}^{4+}$. It is demonstrated by TEM observation and selected area electron diffraction (SAED) patterns that a clear interface between the rhombohedral and pseudocubic phases exists in the interdiffusion layer. The SAED studies also reveal the presence of F spots along the [111] direction of the perovskite cubic unit cell. The origin of this superstructure is determined.
© 2000 Kluwer Academic Publishers

## 1. Introduction

Functionally gradient materials (FGM) are characterized by the compositional and/or microstructural gradation over macroscopic/microscopic distances [1]. With the research and development of the FGM, the scope of which has been extended into other functional materials, such as the piezoelectric ceramic materials, from the initial research aim at obtaining the materials with more advantages in thermal stress relaxation because of the gradient joints within the FGM reducing the residual stresses produced at the interfaces. A typical example is the development of the FGM piezoelectric ceramic actuator to overcome the performance limitations of the usual piezoelectric bimorphs [2]. The FGM piezoelectric ceramic actuator is composed of three layers: a piezoelectric ceramic layer, a high dielectric ceramic layer and a sandwich, whose compositions, microstructures and electrical properties vary gradually. The compositional and microstructural variations of the sandwich (an interdiffusion layer) have great effect on the interfacial bonding strength and the electric-induced displacement characteristics of an FGM piezoelectric actuator [3]. As a consequence, it is necessary to investigate the interdiffusion reaction and the interface structure of the sandwich within the PNN/PZT FGM piezoelectric ceramic actuator before the proceeding conditions of the FGM piezoelectric ceramic actuators

are optimized. In this paper, the compositional profiles, distribution of the phases and short range ordering phenomena in the interdiffusion layer formed in the PNN/PZT interdiffusion couple were investigated by electron probe microbeam analyses (EPMA) and transmission electron microscopy (TEM), respectively.

## 2. Experimental

The interdiffusion couple A-B was constructed by first pressing A powder (composition (mol%): $0.8Pb(Ni_{1/3}Nb_{2/3})O_3$–$0.2Pb(Zr_{0.6}Ti_{0.4})O_3$) in a mould and then adding B powder (composition (mol%): $0.2Pb(Ni_{1/3}Nb_{2/3})O_3$–$0.8Pb(Zr_{0.6}Ti_{0.4})O_3$) and pressing again, both at 30 MPa, to give pellets ($\Phi = 20\,mm$ in diameter) of about 4 mm each in thickness, details in Ref. [4]. In this way, optimal contact between the reactant pellets was assured. The interdiffusion couple was sintered at $1250\,°C$ in air for two hours. The compositional profiles were obtained by EPMA on transverse cuts of the annealed interdiffusion couple. The EPMA experiment was performed in the EPMA-8705QH (Daojin Corp., Japan), operated at 20 kV with $10\,\mu m$ step width.

Specimens for electron microscopy were thinned mechanically and $Ar^+$-ion beam milled after they had been mounted onto 3 mm Mo grids for TEM observation.

---

Samples were coated with carbon before examination in the electron microscope. Structural investigations were carried out with JEM-200CX TEM (JEOL, Japan) operated at 200 kV, using a double-tilt stage.

## 3. Results and discussion

### 3.1. Compositional profiles

The compositional profiles of the diffusion ions obtained after diffusion for two hours at temperature of 1250 °C are shown in Fig. 1. The left side, corresponding to the composition A pellet is taken as zero length. It is revealed that in Fig. 1 the development of the profile along the length perpendicular to the interface shows that a zone of high constant niobate concentration, whereas that of the zirconate is low. At about 550 $\mu$m the niobate concentration starts to decrease and the zirconate one to increase, as expected. A graded region means the interdiffusion layer, which is located between about 550 $\mu$m and 1106 $\mu$m. On the right, a constant concentration of the niobate and zirconate is reached, which corresponds to the initial concentration of the Nb and Zr in composition B. Similar phenomena are also observed in the compositional profiles of the Ni and Ti ions. The normalized concentration profiles for the diffusion ions were simulated numerically by the method described in Ref. [4]. The results are shown in Fig. 2. It is clear that the width of the interdiffusion layer ($d$) controlled by ionic diffusion can be ordered as $d_{Ni}^{2+} > d_{Nb}^{5+} > d_{Ti}^{4+} > d_{Zr}^{4+}$, which implies that the diffusitivities ($D$) of the $Ni^{2+}$, $Nb^{5+}$, $Ti^{4+}$ and $Zr^{4+}$ ions are in the order $D_{Ni}^{2+} > D_{Nb}^{5+} > D_{Ti}^{4+} > D_{Zr}^{4+}$. That can be interpreted as the effects of the ionic radii and valence [4].

### 3.2. Distribution of the phases and short range ordering

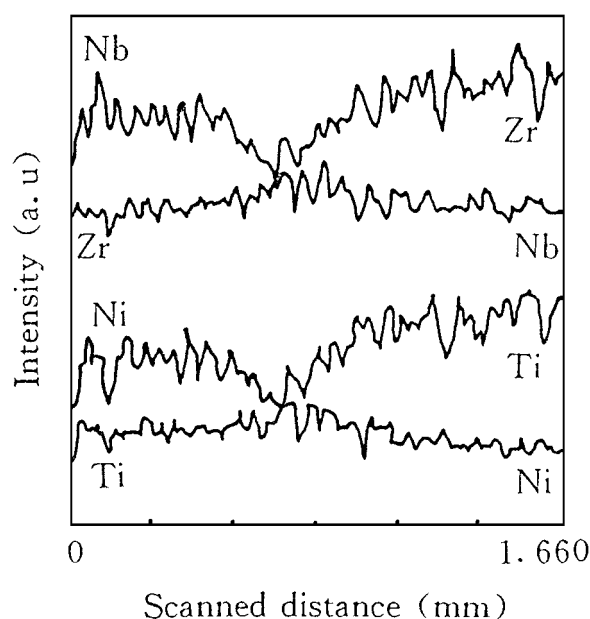The bright-field TEM micrograph of the interdiffusion layer formed in the A-B diffusion couple is shown in



*Figure 1* Compositional profiles of the diffusion ions in the interdiffusion layer formed in the A-B interdiffusion couple at 1250 °C for two hours.

Fig. 3a. It is observed that an interface exists in the interdiffusion layer. To identify the phase structures of the interdiffusion layer, the room temperature ⟨110⟩ zone-axis selected area electron diffraction patterns were taken from the regions marked by I and II in Fig. 3a, which were shown in Fig. 3b and c respectively. In Fig. 3b, splitting from 71° or 109° domains is skewed from the ⟨110⟩, as marked by an arrow, which provides a direct evidence for the existence of the rhombohedral phase on the left side of the interface. It is clear that in Fig. 3c besides the (strong) allowed reflections originating from the cubic perovskite structure, extra (weak) superlattice reflections (F-spots) appear at positions of $(h + \frac{1}{2}, k + \frac{1}{2}, l + \frac{1}{2})$ from the fundamental reflections for a cubic perovskite unit cell with a lattice constant a. The intensity of the superstructure spot along the [111] axes varies from one crystal to another one. The existence of the F-spots clearly confirms that the ordered regions have a doubled perovskite unit cell, as shown in Fig. 4. Similar results are reported for $Pb(Mg_{1/3}Nb_{2/3})O_3$ [5, 6]. Since the average Ni/Nb ratio in the PNN-PZT system is 1 : 2, according to the model proposed by Harmer *et al.* [6, 7], the ordered regions in the present pseudo-ternary system have a Ni : Nb ratio that is 1 : <2, they carry an overall negative charge with respect to the global disordered matrix (Nb-rich), and can be directly charge compensated by the surrounding disordered matrix, which is effectively donor doped since its Ni : Nb ratio is 1 : >2.

In the present PNN-PZT system, the Ni and Nb ions occupy the B-site of the perovskite structure, so as do the Zr and Ti ions from considerations of their ionic radii. Therefore several ionic substitutions can be hypothesized. One possible substitution of Zr ions for Nb ions would lead to a nonstoichiometric 1 : 1 ordering of Ni and Zr ions between two B-site cation sublattices. However such local 1 : 1 short-range ordering of Ni and Zr ions in the PNN-PZT solid solution carries the local B-site valence of +3, which is electrostatically less favorable than the local 1 : 1 ordering of Zr and Nb ions (local valence +4.5) formed by the substitution of Zr for Ni ions on the B-site of perovskite structure. With high valence $Zr^{4+}$ ions replacing the low valence $Ni^{2+}$ ions, such donor doping effect is expected to compensate the charge imbalance resulted from the local 1 : 1 ordering of Ni and Nb ions. That can in turn stabilize the ordered microdomains and promote to increase the degree of the short-range order. Therefore the substitution of Ni ions by Zr ions is much more probable than the substitution of Nb ions by Zr ions.

Since the 1 : 1 order leads to compositional partitioning it is reasonable to expect that the most ordered system will tend to phase separate the earliest [7]. Due to an elastic energy effect, the stability of the 1 : 1 ordering in the $Pb(B'_{1/3}B''_{2/3})O_3$ partly depends upon the size difference of the B-site ions. If a large size difference exists between the B′ and B″ ions, it is believed that the lattice strain is less for the 1 : 1 ordering than for disordering or 1 : 2 stoichiometric ordering [6]. The ionic size difference between the $Zr^{4+}$ and $Nb^{5+}$ ions on the B-site of the perovskite structure (coordination number 6) is 0.008 nm [8], and this value is greater
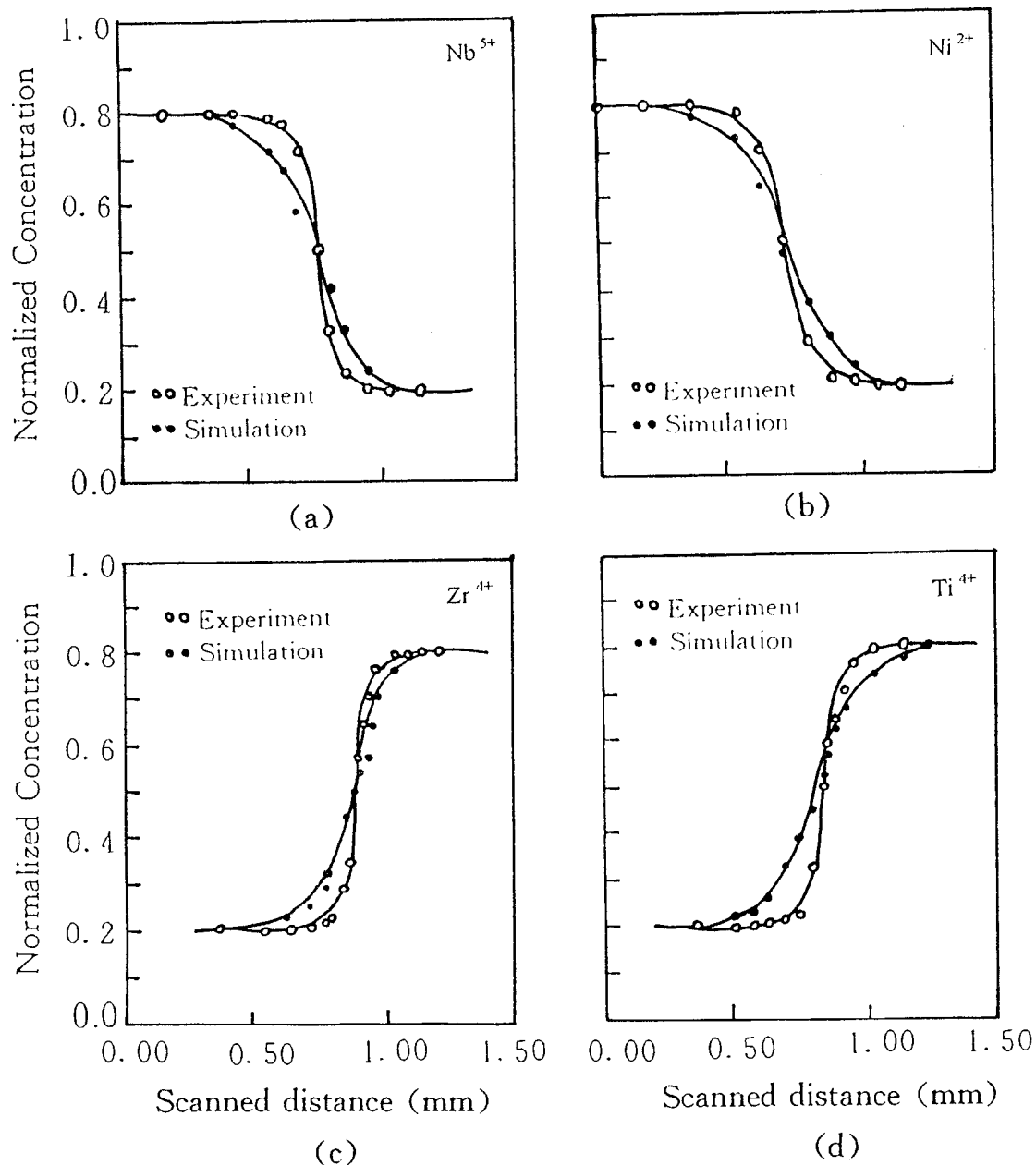
*Figure 2* Normalized concentration profiles simulated numerically for the diffusion ions, and compared to that obtained from the EPMA experiment (diffusion conditions: 1250 °C/2 hrs).

than the difference between the $Ni^{2+}$ and $Nb^{5+}$ ions (0.005 nm) [8]. Therefore the stability of the 1 : 1 Nb-Zr short-range ordering is much higher than that of the 1 : 1 Ni-Nb short-range ordering. Consideration of the possible 1 : 1 ordering of Ni and Ti ions yields an average valence of +3 on B-site and is therefore electrostatically less favorable than the Ni:Nb order. The Nb:Ti order is also unlikely since this type of 1 : 1 ordering involves the substitution of the small-sized Ti ion for the relatively large-sized Ni ion which requires less favorable strain energy than the Ni:Nb ordering ($R_{Ni}^{2+} = 0.069$ nm, $R_{Ti}^{4+} = 0.0605$ nm) [8]. Ti ions are believed to dilute the forces responsible for the ordering process [9]. The degree of the B-site 1 : 1 order is decreased with increasing the PT content, which is identified by

the PT content dependence of the domain morphologies for the $0.2Pb(Ni_{1/3}Nb_{2/3})O_3–0.8Pb(Zr_{1-x}Ti_x)O_3$ samples. Fig. 5a–c illustrate the dependence of the room-temperature bright field image on PT content in the $0.2Pb(Ni_{1/3}Nb_{2/3})O_3–0.8Pb(Zr_{1-x}Ti_x)O_3$ specimens for composition $x = 0.30$, 0.50 and 0.60, respectively. It is revealed that in the rhombohedral-rich side ($x = 0.30$), only local random contrast representing short-range order polar clusters or nanodomains is observed, and no evidence of micro-sized domains is found. For compositions near the PNN-PZ-PT morphotropic phase boundary ($x = 0.50$), normal micron-sized domains appear, and become stable in the tetragonal-rich field ($x = 0.60$), in which a well-defined 90° ferroelectric macro-domains can readily be seen.
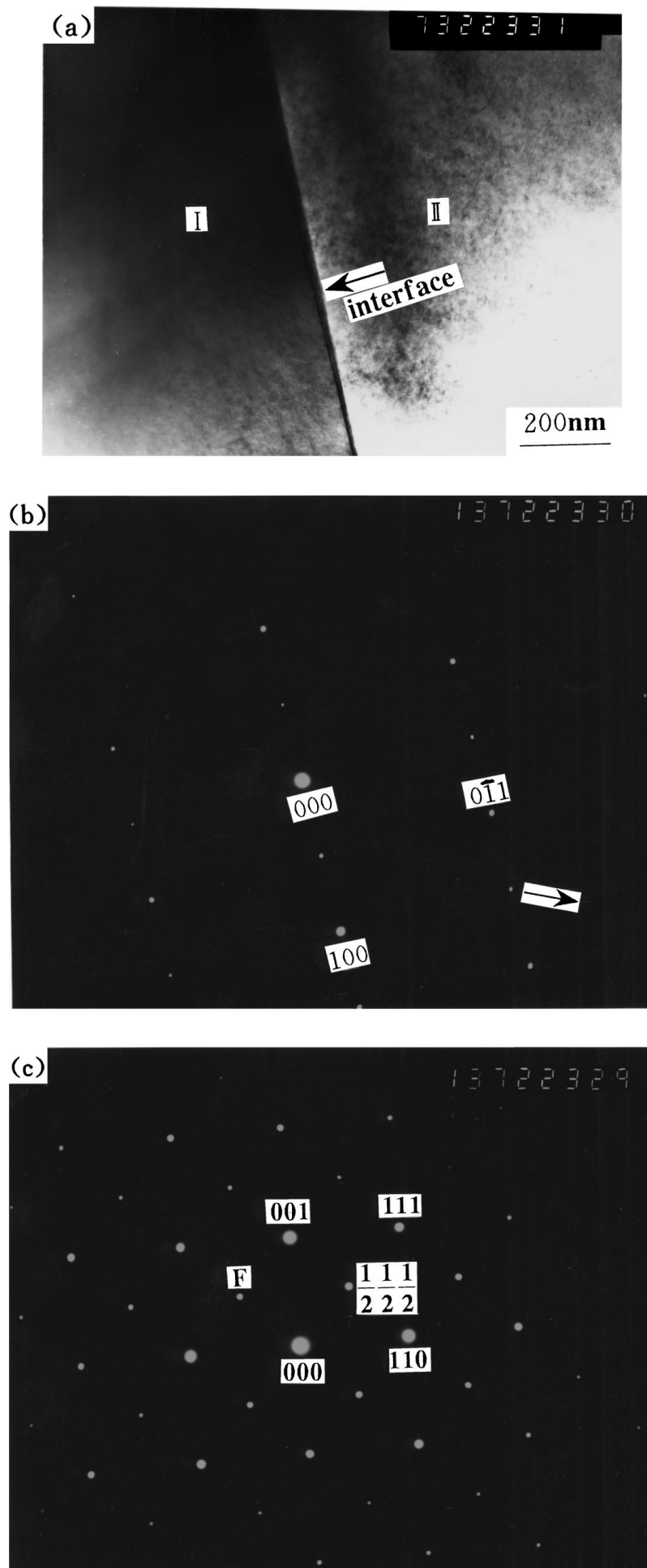
*Figure 3* (a) Bright-field TEM micrograph of the interdiffusion layer formed in the A-B diffusion couple at room temperature, (b) and (c) for the room temperature ⟨110⟩ zone-axis selected area electron diffraction patterns taken from the regions marked by I and II in Fig. 3a, respectively.

Based on the facts discussed above, it can be concluded that the phase structures of the interdiffusion layer formed in the PNN-PZT system are composed of the rhombohedral and pseudocubic phases. The $\frac{1}{2}[111]$ superlattice refle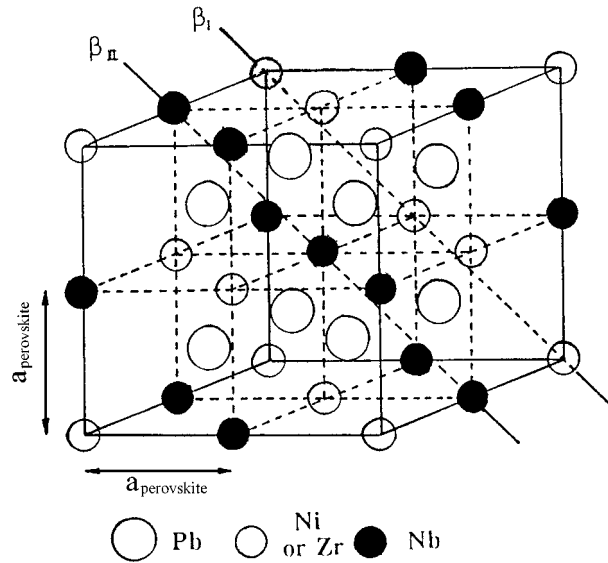ctions (F-spots) are originated from the enhanced short-range, non-stoichiometric 1 : 1 ordering of the Zr and Nb cations.

## 4. Conclusions

Using the EPMA and TEM techniques the compositional profiles, distribution of the phase and short-range ordering of the interdiffusion layer formed in the PNN/PZT functionally gradient piezoelectric ceramics have been investigated. It is found that the thickness of the interdiffusion layer ($d$) of the $Ni^{2+}$, $Nb^{5+}$, $Ti^{4+}$ and $Zr^{4+}$ ions decreases in the order $d_{Ni}^{2+} > d_{Nb}^{5+} > d_{Ti}^{4+} > d_{Zr}^{4+}$. A clear interface between the rhombohedral and pseudocubic phases exists in the interdiffusion layer. The $\frac{1}{2}[111]$ superlattice spots (F-spots) are originated from the enhanced short-range, non-stoichiometric 1 : 1 ordering of the Zr and Nb cations on an F-centred superlattices, whose intensities vary from one crystal to another one along the [111] axes.



*Figure 4* Proposed model for the atomic configuration of the $\frac{1}{2}\{111\}$-ordered structure in the PNN-PZT crystalline solution, illustrating the formation of two distinct B-site cation sublattice. $\beta_I$ and $\beta_{II}$ for nickel (or zirconate) and niobium respecrively.

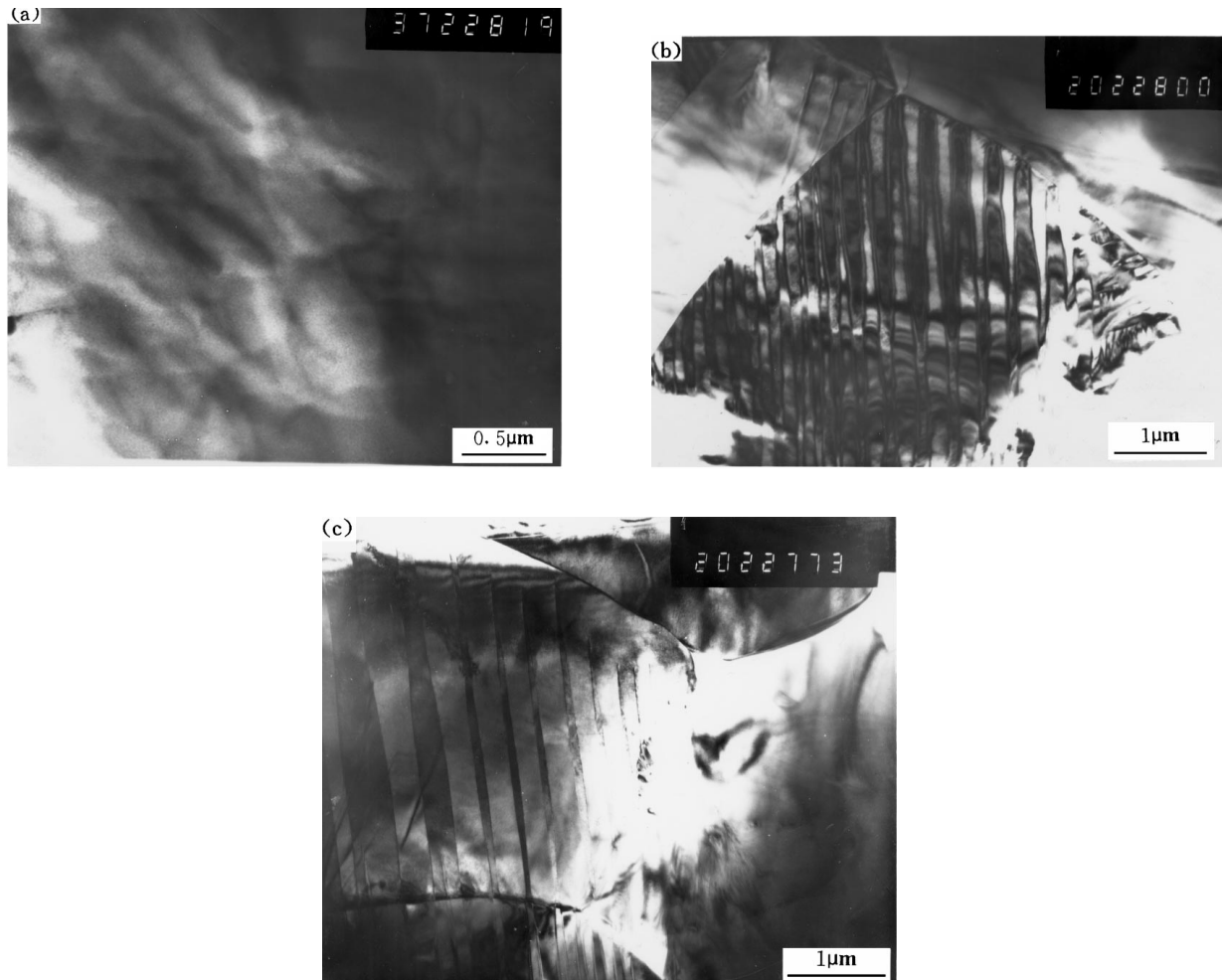*Figure 5* Bright-field TEM micrographs at room temperature showing the domain morphologies of the $0.2Pb(Ni_{1/3}Nb_{2/3})O_3-0.8Pb(Zr_{1-x}Ti_x)O_3$ samples for compositions (a) $x = 0.30$, (b) $x = 0.50$, and (c) $x = 0.60$, respectively.

## References

1. N. CHERRADI, A. KAWASAKI and M. GASIK, *Composites Engineering* **4** (1994) 883.
2. X. H. ZHU, Q. WANG and Z. Y. MENG, *J. Mater. Sci. Lett.* **14** (1995) 516.
3. X. H. ZHU and Z. Y. MENG, *Sensors & Actuators A: Physical,* **48** (1995) 169.
4. X. H. ZHU, J. XU and Z. Y. MENG, *J. Mater. Sci.* **33** (1998) 1023.
5. C. A. RANDAL and A. S. BHALLA, *Jpn. J. Appl. Phys.* **29** (1990) 327.
6. J. CHEN, H. CHAN and M. P. HARMER, *J. Amer. Ceram. Soc.* **72** (1989) 593.
7. M. P. HARMER, J. CHEN, P. PENG, H. M. CHAN and D. M. SMYTH, *Ferroelectrics* **97** (1989) 263.
8. R. D. SHANNON, *Acta. Cryst. A* **32** (1976) 751.
9. A. D. HILTON, D. J. BARBER, C. A. RANDALL and T. R. SHROUT, *J. Mater. Sci.* **25** (1990) 3461.